

# The confinement effect on the activity of Au NPs in polyols oxidation

Cite this: DOI: 10.1039/x0xx00000x

Alberto Villa,<sup>a</sup> Di Wang,<sup>b</sup> Carine E. Chan-Thaw<sup>a</sup>, Sebastiano Campisi<sup>a</sup>, Gabriel M. Veith<sup>c</sup> and Laura Prati<sup>a,\*</sup>

Received 00th January 2012,

Accepted 00th January 2012

DOI: 10.1039/x0xx00000x

www.rsc.org/

**We demonstrate a confinement effect where gold nanoparticles trapped within N-functionalized carbon nanofibers (N-CNFs) are more active for polyol oxidation and promote selectivity towards di-acid products whereas AuNPs trapped on the surface show as major by-products the one derived from C-C cleavage. The behaviour of NPs confined inside N-CNFs channels can be addressed to a different, possibly multiple, coordination of glycerol on the active site.**

In recent years gold based catalyst have attracted broad interest for the catalytic transformation of biomass derived chemicals.<sup>1</sup> For example, gold catalysts were found very active for the liquid phase oxidation of glycerol to high value products such as glyceric acid (GLYA), dihydroxyacetone (DHA) and tartronic acid (TA).<sup>1c,2</sup> A large number of experiments have shown that, in this reaction, the catalytic activity and selectivity are highly dependent on the size and the structure of AuNPs.<sup>3</sup> Through optimizing the AuNPs size it is possible to enhance the selectivity to glyceric acid limiting the production of degradation products due to C-C cleavage.<sup>3</sup> Selectivity can be also optimized by controlling the exposed Au faces.<sup>4</sup> Moreover, it has been demonstrated that the morphology and the surface chemistry of the support can alter the catalytic performance of AuNPs.<sup>5</sup> The introduction of oxygen or nitrogen functionalities on carbon nanofibers can enhance the catalytic activity, increasing the AuNPs dispersion but also modifying the electronic surface state.<sup>6</sup> One thing all these studies have in common is that the gold nanoparticles were supported on the exterior of the catalyst support. In this work we aim to explore the role of gold location, i.e. gold located within or on the outside of the support, and the influence of the location on the catalytic performance.

One material which could help answer this question are carbon nanofibers (CNFs) which have well defined tubular structures within the core of the fiber (20-50 nm diameter).<sup>7</sup> Different strategies have been used to selectively deposit metal nanoparticles in or outside carbon nanotubes and carbon nanofibers with a significant effect of their catalytic performance in both gas and liquid phase reactions.<sup>7</sup>

For example, Serp et al. showed that PtRu nanoparticles inside carbon nanotubes are more active than the ones deposited on the external surface in the cinnamaldehyde hydrogenation.<sup>8</sup> Wang et al, proved that the confinement of Ru inside carbon nanotubes influences the selectivity during cinnamaldehyde, benzene and p-chloronitrobenzene hydrogenation due to an electronic effect.<sup>7c</sup> In this paper, the effect of the location of AuNPs was investigated in the liquid phase glycerol oxidation.

To increase metal dispersion and stability against leaching nitrogen heteroatoms were added to the CNF surface to act as anchoring groups for the metal nanoparticles regardless the procedure used for the preparation of metal nanoparticles.<sup>6</sup> Nitrogen species were added using a two-step procedure described elsewhere.<sup>9</sup> N1s XPS data collected for the functionalized CNFs (Table S1, [Figure S1a](#)) showed three distinct N species with binding energies of 398.6, 400.5 and 404.2 eV consistent with pyridinic (51.3%), pyrrolic N (40.7%) and NO species (8.0%), respectively. The total amount of N introduced was 4.5 % wt (Table S1, [Figure S1a](#)).

Two different strategies were adopted to prepare Au nanoparticles, i.e. sol immobilization (SI) and incipient wetness impregnation (IW). SI was used to limit the deposition of AuNPs on the external surface of N-CNFs. The presence of the capping agent (polyvinyl alcohol, PVA) increases the hydrodynamic radius of the particles, thus limiting their internal diffusion inside the channel. On the contrary, incipient wetness impregnation forces the Au precursor to enter the N-CNF channel, interacting mainly with the inner surface. In the case of sol immobilization, in order to remove PVA from AuNP surface, the catalyst was thoroughly washed with warm water. Indeed it has been reported that the presence of the protective agent can decrease Au catalytic performance by blocking the active sites but also alter the reaction selectivity.<sup>10</sup> STEM measurements show in both catalysts the presence of small nanoparticles with a similar mean diameters between 3.2-3.4 nm (Table S2 and Figure 1) and particles distribution ([Figure S2](#)). This STEM data also show that the Au is well dispersed on the support in both cases, confirming the

beneficial effect of the functionalization with nitrogen groups. HRTEM images (Figures 2) showed that in both cases Au surface is almost free from amorphous carbon thus presenting naked metallic surface.

HAADF STEM electron tomography was used to study the 3D structure of carbon nanofiber supported Au catalysts obtained by the two different synthetic procedures. HAADF STEM tomogram was reconstructed from tilt series images in a tilting angle range between at least  $\pm 70^\circ$  with a step of  $2^\circ$ . After reconstruction, the cross-sectional slices intersecting a few particles on one representative N-CNFs for each catalyst were shown in Figure 3 and Figures S3-S4. For the impregnated  $\text{Au}_{\text{Iw}}/\text{N-CNFs}$ , majority of particles were found inside the N-CNFs, even some particles were on the external surface as well (Figure 3a). The different location of Au nanoparticles has been also confirmed by XPS (Table S1, Figure S1b,c). Indeed, a reduction in Au intensity of the  $\text{Au}_{\text{Iw}}$  sample compared to that of the  $\text{Au}_{\text{SI}}$  material despite the identical 1 wt% metal loadings and similar size (XPS signal=2.8 at% Au for  $\text{Au}_{\text{SI}}/\text{N-CNFs}$ ; 0.1 at% for  $\text{Au}_{\text{Iw}}/\text{N-CNFs}$ ; Table S1, Figure S1b,c) was observed.

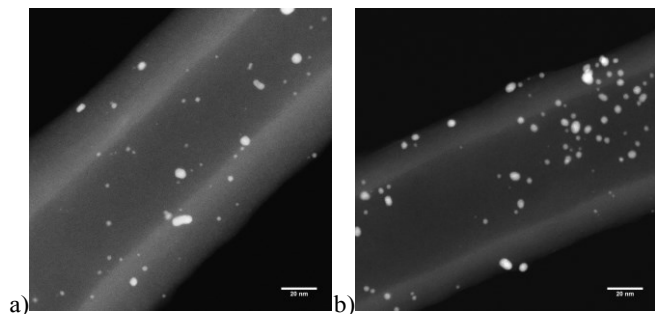


Figure 1 STEM images of a)  $\text{Au}_{\text{Iw}}/\text{N-CNFs}$  and b)  $\text{Au}_{\text{SI}}/\text{N-CNFs}$

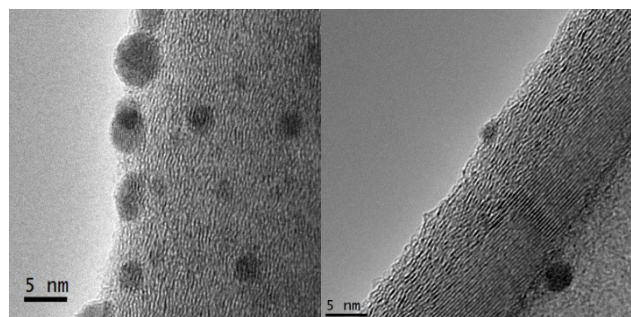


Figure 2 HRTEM images of a)  $\text{Au}_{\text{SI}}/\text{N-CNFs}$  and b)  $\text{Au}_{\text{Iw}}/\text{N-CNFs}$

The catalysts were first tested in the glycerol oxidation at  $50^\circ\text{C}$  (0.3M glycerol, glycerol/metal=1000 mol/mol, 3 atm  $\text{O}_2$ , 4eq of NaOH) (Table 1).  $\text{Au}_{\text{Iw}}/\text{N-CNFs}$  showed a better activity than  $\text{Au}_{\text{SI}}/\text{N-CNFs}$  reaching 92% and 78% of conversion after 1h, respectively (Table 1 and Figure S5) and also an almost double initial activity with respect to  $\text{Au}_{\text{SI}}/\text{N-CNFs}$  (1521 and 864 mol of glycerol converted per hour per mol of metal, respectively). In a previous paper we showed that the presence of residual capping

agent can decrease the catalytic activity limiting the access of the substrate to Au active sites.<sup>10</sup> However in this case PVA has been removed from the catalyst surface by washing several times with water, as confirmed from the HRTEM image of  $\text{Au}_{\text{SI}}/\text{N-CNFs}$  (Fig. 2a).

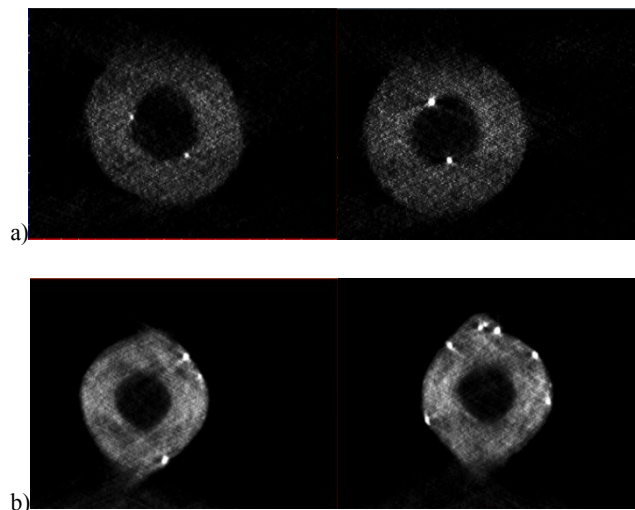


Figure 3 Cross sectional slices derived from electron tomography showing a) Au particles prepared by impregnation situated on both inner- and outer-surfaces of CNF and b) preformed  $\text{Au}_{\text{SI}}$  particles exclusively situated on the outer surface of CNF.

Moreover, both catalysts Au showed similar mean diameter (3.2-3.4 nm) excluding any role in term of AuNPs size.

Table 1. Oxidation of glycerol using Au supported catalysts<sup>a</sup>

Catalyst <sup>a</sup>	Time (h)	Conv. (%)	Selectivity (%)			
			GLYA	TA	GLYCA	FA
$\text{Au}_{\text{Iw}}/\text{N-CNFs}$	0.25	38	65	25	5	2
	0.5	61	64	28	6	2
	1	92	62	27	7	3
$\text{Au}_{\text{SI}}/\text{N-CNFs}$	0.25	20	73	11	10	4
	0.5	43	69	12	12	5
	1	78	66	11	15	6
	1.5	91	64	11	17	8

<sup>a</sup> Glycerol 0.3M in water; 4eq of NaOH; metal/alcohol = 1/1000 mol/mol; 3 atm  $\text{O}_2$ ; T= $50^\circ\text{C}$ .

GLYA=glyceric acid; TA=tartronic acid; GLYCA=glycolic acid; FA= formic acid

Therefore a possible reason for the increase in catalytic activity could lie on the confinements effect of Au inside the CNFs channel as found for Pt-Ru, Pt or Pd nanoparticles inside carbon nanotubes.<sup>7,8,11,12</sup> Theoretical studies on confined metal nanoparticles showed that the catalytic activity can be influenced by an enlarged number of collisions of the substrate with the active site due to the reduced reaction volume inside the channels.<sup>13</sup> It has been also demonstrated the activity of metal nanoparticles can be influenced by an electronic effect induced by the confinement inside the channels.<sup>7b,c</sup> For example, it was shown that the activity of Ru NPs in cinnamaldehyde hydrogenation is influenced by the different electron transfer between reactants and catalysts according to their location inside or outside CNFs.<sup>7e</sup>

In the case of our catalysts we observed a strong effect on both activity and selectivity. At iso-conversion (90%) Au<sub>IW</sub>/N-CNFs and Au<sub>SI</sub>/N-CNFs showed a similar selectivity to glycerate (62-64%) (Table 1). However, a difference has been observed for the other products. Au<sub>IW</sub>/N-CNFs promotes the formation of tartronate (27% with respect to 11% of Au<sub>SI</sub>) deriving from the consecutive oxidation of glycerate whereas Au<sub>SI</sub>/N-CNFs presents a higher tendency to promote the cleavage of C-C forming glycolate (17% with respect of 7% of Au<sub>IW</sub>). This is quite unusual for gold catalysts which tend to selectively stop at the oxidation of only one alcoholic function.<sup>14</sup> Considering the possible reaction scheme (Scheme S1) we could not ascribe this different behaviour to a different residence time of the reactant inside the pores because of the reaction rate is very similar in the two cases. Most probably a different adsorption mode of glycerol can be experimented by the active sites on the inner surface. On the opposite, the outer active sites do not suffer from any constrains in adsorption and the reaction proceed to glycolate.

The long-term stability of both catalysts was investigated using recycling tests (Table S3 and S4) carried out by filtering the catalyst and reusing it without any further purification in the next run. Both catalysts showed a good stability in terms of both activity and selectivity, regardless the location of Au NPs. Probably the nitrogen functionalities introduced are able to firmly anchored Au NPs avoiding any leaching and reconstruction excluding any modification of the catalyst morphology during the reaction. Extending the catalytic test to other polyols, 1,3 propanediol and ethylene glycol, the trend observed for glycerol oxidation was confirmed (Table S5). In both cases Au<sub>IW</sub>/CNFs resulted more active than Au<sub>SI</sub>/CNFs and promote the oxidation of both OH groups producing malonate and oxalate respectively (Table S5).

## Conclusions

Herein we showed that the location of Au NPs has a strong effect on their catalytic activity and selectivity in the liquid phase polyols oxidation. By means of sol immobilization technique we were able to deposit AuNPs only on the external surface of CNFs, whereas incipient wetness impregnation provided AuNPs almost quantitatively inside the pores. The preferential location of Au NPs was confirmed by studies performed using electron tomography in HAADF STEM mode. The confinement of Au NPs significantly enhances the catalytic

activity and modifies the selectivity normally observed for gold catalyst in polyol oxidation, promoting the oxidation of both functionalities. This behaviour has been addressed to the higher number of collisions and to a different electron density of Au nanoparticles and to a modified desorption rate of the primary product.

## Notes and references

<sup>a</sup> Dipartimento di Chimica, Università degli Studi di Milano, via Golgi 19, 20133 Milano, Italy.

\* Email: Laura.Prati@unimi.it

<sup>b</sup> Institute of Nanotechnology and Karlsruhe Nano Micro Facility, Karlsruhe Institute of Technology, Hermann-von-Helmholtz-Platz 1, 76344 Eggenstein-Leopoldshafen, Germany.

<sup>c</sup> Materials Science and Technology Division Oak Ridge National Laboratory Oak Ridge, TN 37831 (USA).

Electronic Supplementary Information (ESI) available: [Experimental details, XPS data, and additional catalytic results]. See DOI: 10.1039/c000000x/

- 1 a) N. Dimitratos, J. A. Lopez-Sanchez, G. J. Hutchings, *Chem. Sci.*, 2012, 3, 20. b) S. E. Davis, M. S. Ide, R. J. Davis, *Green Chem.* 2013, 15, 17; c) A. Villa, N. Dimitratos, C. E. Chan-Thaw, C. Hammond, L. Prati, and G. J. Hutchings, *Acc.Chem.Res.* 2015, 48, 1403 Sankar, M.; Dimitratos, N.; Miedziak, P. J.; Wells, P. P.; Kiely, C. J.; Hutchings, G. J. *Chem. Soc. Rev.* 2012, 41, 8099-8139.
- 2 a) Carrettin, S.; McMorn, P.; Johnston, P.; Griffin, K.; Hutchings, G.J. *Chem. Commun.* 2002, 696. b) Zope, B.N.; Hibbits, D. D.; Neurock, M.; Davis, R. J. *Science*, 2010, 330, 74-78. c) Porta, F.; Prati, L. *Selective J. Catal.* 2004, 224, 397-403. c) Villa, A.; Campisi, S.; Mohammed, K. M. H.; Dimitratos, N.; Vindigni, F.; Manzoli, M.; Jones, W.; Bowker, M.; Hutchings, G. J.; Prati, L. *Catal. Sci. Tech.* 2015, 5, 1126-1132.
- 3 a) Porta, F.; Prati, L. *J. Catal.* 2004, 224, 397-403 b) S. Demirel-Gulen, M. Lucas, P. Claus, *Catal. Today*, 2005, 102-103, 166. c) Ketchie, W. C.; Fang, Y.; Wong, M. S.; Murayama, M.; Davis, R. J. *J. Catal.* 2007, 250, 94-101.
- 4 Wang, D.; Villa, A.; Su, D.; Prati, L.; Schloegl, R. *ChemCatChem* 2013, 5, 2717-2723.
- 5 Villa, A.; Veith, G. M.; Ferri, D.; Weidenkaff, A.; Perry, K. A.; Campisi, S.; Prati, L. *Catal. Sci. Technol.*, 2013, 3, 394-399. Villa, A.; Veith, G.M.; Prati, L. *Angew. Chem. Int. Ed.* 2010, 49, 4499-4502. Brett, G. L.; He, Q.; Hammond, C.; Miedziak, P. J.; Dimitratos, N.; Sankar, M.; Herzog, A. A.; Conte, M.; Lopez-Sanchez, J. A.; Kiely, C. J.; Knight, D. W.; Taylor, S. H.; Hutchings, G. J. *Angew. Chem. Int. Ed.* 2011, 50, 10136-10139.
- 6 Prati, L.; Villa, A.; Chan-Thaw, C.E.; Arrigo, R.; Wang D.; Su, D.S. *Faraday Discuss.* 2011, 152, 353-365.
- 7 a) X. Pan, X. Bao, *Chem. Comm* 2008, 6271; J. P. Tessonnier, O. Ersen, G. Weinberg, C. Pham-Huu, D. S. Su, R. Schloegl, *ACS Nano*, 2009, 3, 2081; b) P.Serp, E. Castillejos, *ChemCatChem.*, 2010, 2, 41; c) X. Pan, X. Bao, *Acc. Chem.*

- Res. , 2011, 44, 553.; e) Y. Wang, Z. Rong, Y. Wang, P. Zhang, Y. Wang, J. Qu, *J Catal.*, 2015, 329, 95.
- 8 E. Castillejos, P-J. Debouttier L. Roiboan, A. Solhy, V. Martines, Y. Kihn, O. Ersen, K. Philippot, B. Chaudret, P. Serp, *Angew. Chem Int. Ed.* 2009, 121, 2567.
  - 9 R. Arrigo, M. Hävecker, R. Schlögl, D. S. Su, *Chem. Commun.* 2008, 4891-4893
  - 10 A. Villa, D. Wang, G.M. Veith, F. Vindigni, F.; Prati, L. *Catal. Sci. Technol.* 2013, 3, 3036-3041.
  - 11 H. Ma, L. Wang, L. Chen, C. Dong, W. Yu, T. Huang, Y. Qian, *Catal. Commun.* 2007, 8, 452–456.;
  - 12 J.-P. Tessonier, L. Pesant, G. Ehret, M. J. Ledoux, C. Pham-Huu, *Appl. Catal. A: Gen.* 2005, 288, 203 –210.
  - 13 E. E. Santiso, M. K. Kostov, A. M. George, M. Buongiorno Nardelli, K. E. Gubbins. *Appl. Surf. Sci.* 2007, 253, 5570 – 5579. b) T. Lu, E. M. Goldfield, *J. Phys. Chem. C* 2008, 112, 2654 –2659. C) M. D. Halls, H. B. Schlegel, *J. Phys. Chem. B*, 2002, 106, 1921 –1925.
  - 14 A. Villa, D. Wang, G. M. Veith, L. Prati, *J. Catal.* 2012, 292 73-80